CILAMCE 2017
Florianópolis - Santa Catarina - Brazil

MULTISCALE STRATEGY FOR THE ANALYSIS OF SOFTENING MEDIA USING THE GENERALIZED FINITE ELEMENT METHOD

Humberto Alves da Silveira Monteiro

humberto@dees.ufmg.br

Roque Luiz da Silva Pitangueira

roque@dees.ufmg.br

Felício Bruzzi Barros

felicio@dees.ufmg.br

Department of Structural Engineering, Federal University of Minas Gerais

Av. Antônio Carlos 6627, 31270-901, Belo Horizonte, MG, Brazil

Abstract. *All the materials are heterogeneous in some sufficiently small length scale and in the case of quasi-brittle media it is exactly the inhomogeneous nature of the continuum that accounts for many of the phenomena captured in structural level, especially the prominent non-linear mechanical behavior. In that sense, this work proposes the adoption of the Generalized Finite Element Method associated with the Global-Local methodology (GFEM-GL) to build a different multiscale strategy able to model general strain softening materials, especially quasi-brittle media and its main archetype, the concrete. In an incremental-iterative scheme, the solution of an initial global boundary value problem (macroscale) generates boundary conditions to local domains (mesoscale). Then the solution of the inhomogeneous local problems numerically creates enrichment functions for the global domain and the constitutive response of the non-linear material. Lastly, the enriched global problem is processed again. At the current stage, the material morphology has been modeled using a stochastic-heuristic algorithm and numerically treated by the Finite Element Method, one of the many possible options to handle the local/meso problem. The work has been carried out within the INSANE system (INteractive Structural Analysis Environment), a free software developed at the Federal University of Minas Gerais-Brazil.*

Keywords: *Generalized Finite Element Method, Multiscale Analysis, Mesostructure, Softening and Non Linear Analysis*

1 INTRODUCTION

Materials formed by dissimilar constituents distinguishable in a certain length scale, small by definition, are called heterogeneous, non-homogeneous, microstructured or complex. Common examples are: generic composites, concrete, polycrystals, polymers, cellular solids, biological tissues, wood, soil, clay, foams, among others. Due to the nature of their fracture, some of these materials, such as concrete and geomaterials, can be classified as quasi-brittle (Bohm, 2016; Fuina et al., 2010).

Quasi-brittle media are those which exhibit moderate hardening prior their ultimate tensile strength is reached. After this peak, the increasing of strains happens in parallel to the decreasing of stresses (strain softening). This behavior, markedly non-linear, is directly related to micromechanical aspects of the material, in which the heterogeneity is one of the predominant causes (Karihaloo, 2010).

In general, the behavior of materials and structures is studied by using single-scale models, representing the macroscopic level. In these models, phenomenological constitutive equations are used to capture the behavior of the underlying (refined) scales. As an alternative to this single (macroscopic) scale approach, multiscale modeling can be adopted to capture the relevant physical phenomena of different observation levels. This approach does not eliminate the use of phenomenological constitutive equations at lower scales, except when it is at the atomistic level. Indeed, it can face – to some extent – certain uncertainties incorporated in many of the single-scale constitutive models (Zienkiewicz et al., 2006).

In computational mechanics, the use of numerical methods is notoriously one of the main tools in the study of materials and structures, being the Finite Element Method (FEM) the most popular one. More recently, the Generalized Finite Element Method (GFEM) has been developed in several scientific studies (Duarte et al., 2000; Duarte, 2001; Duarte and Babuška, 2005; Duarte and Kim, 2008; Gupta et al., 2015; Barros, 2002) to solve various solid mechanics problems, especially those of fracture. In this method, the original approximation space of a finite element is enriched by special functions, in order to capture specific phenomena.

Currently, the GFEM is used in problems of more than one scale of analysis (Kim et al., 2009; Kim and Duarte, 2009; Kim et al., 2010, 2012; Kim and Duarte, 2015; Plews and Duarte, 2014, 2016; Alves, 2012) in which one seeks to investigate the behavior of local (refined) domains that have singularities or some other peculiarity, as well as to study the global (coarse) domains. In this context, the Generalized Finite Element Method with Global-Local Enrichment (GFEM-GL) emerges, using enrichment functions derived from a hybrid composition of the traditional Global-Local analysis (Noor, 1986; Ransom and N. F. Knight, 1989) and GFEM.

The study of materials with hierarchical structure may improve the knowledge on media with specific special properties, used in several engineering applications, due to the understanding of the individual behavior of its components and the interaction between them.

In that sense, this work proposes the adoption of the GFEM-GL to model quasi-brittle (softening) media with the introduction of the material heterogeneity, and therefore, following a multiple scale approach, more specifically one with two levels: one macroscopic or structural scale and one mesoscopic scale – in which the morphology of the medium will be described. In order to do so, the INSANE System (INteractive Structural ANalysis Environment), a free software developed in the Department of Structural Engineering of the Federal University of Minas

Gerais, written in Java language and available at `http://www.insane.de.ufmg.br`, is employed. The system is composed by interactive-graphical applications of pre- and post-processing that work together with a numerical core, which has implementations of standard FEM, GFEM, GFEM-GL (linear case), Boundary Element Method, Meshless Methods, non-linear analysis, as well as a wide range of constitutive models, structured in the Unified Environment for Constitutive Models (Gori et al., 2017). We expect that the proposed methodology in this paper could be used not only to expand the numerical core of INSANE, but could also be able to model the softening behavior of some materials by applying a general multiscale strategy to GFEM, enabling one to get the overall domain response and a more detailed internal description of the material behavior. In the current stage of the work, the researchers present a material morphology generator of particulate media implemented to describe the internal composition and geometry of the analysis domain. These aspects and results are crucial to future achievements, as they consist in one of the most natural ways to handle the material heterogeneity and a important option to describe the mesoscopic problem, since their visual and physical appeals are very prominent.

In the following, we have: in Section 2, the fundamentals of the Generalized Finite Element Method and its association with the Global-Local methodology are presented. Then, in Section 3, the theoretical multiscale strategy proposed here is registered together with some operational aspects. In Section 4, the current research stage is presented and the treatment of the morphology of a typical particulate material is shown, which will take part in the future implementation of the proposed nonlinear analysis. At the end, final considerations are presented in Section 5.

2 GENERALIZED FINITE ELEMENT METHOD

The Generalized Finite Element Method (GFEM) is a relatively new numerical method, developed in the mid-1990s. It originally refers to the work of Babuška et al. (1994), named as Special Finite Element Method, and Melenk and Babuška (1996), referenced as Partition of Unity Method (PUM). These theories were developed in parallel to the formulation of some meshless methods (more specifically, the hp-Cloud Method of Duarte and Oden (1996*a*,*b*) and Duarte (1995). According to Barros (2002), its use under its current terminology have first appeared in Melenk (1995). It is noteworthy that the extrinsic enrichment strategy of the GFEM is similar to that one used by another numerical method, the Extended Finite Element Method (XFEM). According to Fries and Belytschko (2010), the nomenclature distinction between PUM, GFEM and XFEM has become very confusing, and in practice, they may be considered identical or equivalent methods.

2.1 Formulation

Let Ω be a generic domain and Ω^h its partition of unity by standard finite elements, in which Ω^h is the union of individual elements Ω^e, with $e = 1, \ldots, n^e$; $n^e =$ *total number of elements*. One could specify three main components of the GFEM approximation space:

1. *Clouds or Patches (ω_α)*: Union of finite elements which have node α as incidence. Therefore, the set $\{\omega_\alpha\}_{\alpha=1}^{n}$, *n = number of nodes*, is a open cover such as $\Omega^h = \bigcup_{\alpha=1}^{n} \omega_\alpha$.
2. *Partition of Unity (PU) subjected to the cover $\{\omega_\alpha\}_{\alpha=1}^{n}$*: Basically, a PU is a set of functions which sum the unity in whichever point $\mathbf{x}$ belonging to the domain Ω^h. In that sense, the FEM shape functions, N_α, $\alpha = 1, \ldots, n$, compose a PU, i.e., $\sum_{\alpha=1}^{n} N_\alpha(\mathbf{x}) = 1 \;\forall\; \mathbf{x} \in \Omega^h$.

3. *Approximation spaces χ_α of the clouds*: To every cloud, there is a set χ_α, with dimension $D(\alpha)$, of functions $L_{\alpha i}$, so that $\chi_\alpha = \{L_{\alpha i}, 1 \leq i \leq D(\alpha), L_{\alpha i} \in H^1(\omega_\alpha)\}$. To the base functions $L_{\alpha i}$ we give the name *enrichment functions*. $L_{\alpha i}$ could be polynomial, singular, discontinuous (among others), depending on the studied problem.

Thus, the GFEM approximation space ($\mathbb{S}_{GFEM}$) is obtained by the hierarchical expansion of the approximation space of the traditional Finite Element Method ($\mathbb{S}_{FEM}$), using the space corresponding to the enrichment ($\mathbb{S}_{ENR}$), that is:

$$\mathbb{S}_{GFEM} = \mathbb{S}_{FEM} + \mathbb{S}_{ENR} \tag{1}$$

in which

$$\mathbb{S}_{FEM} = \sum_{\alpha \in I} N_\alpha(\mathbf{x}) a_\alpha \tag{2}$$

$$\mathbb{S}_{ENR} = \sum_{\alpha \in I_{ENR}} N_\alpha(\mathbf{x}) \chi_\alpha; \text{ with } \chi_\alpha = \sum_{i}^{n_{ENR}} L_{\alpha i}(\mathbf{x}) b_{\alpha i} \tag{3}$$

where I is the FEM nodal indexes set; $I_{ENR} \subset I$ is the enriched nodes indexes set and n_{ENR} is the total number of nodes; a_α and $b_{\alpha i}$ are nodal values of quantities approximated in each space.

The shape functions in $\mathbb{S}_{GFEM}$ are computed by:

$$\phi_{\alpha i}(\mathbf{x}) = N_\alpha(\mathbf{x}) L_{\alpha i}(\mathbf{x}) \tag{4}$$

Finally, a generic scalar field u could be approximated by the GFEM following equation 5, i.e.:

$$u(\mathbf{x}) \approx \tilde{u}(\mathbf{x}) = \sum_{\alpha \in I} N_\alpha(\mathbf{x}) a_\alpha + \sum_{\alpha \in I_{ENR}} N_\alpha(\mathbf{x}) \sum_{i}^{n_{ENR}} L_{\alpha i}(\mathbf{x}) b_{\alpha i}; \;\; \mathbf{x} \in \Omega^h \text{ and } a_\alpha, b_{\alpha i} \in \mathbb{R} \tag{5}$$

2.2 Global-local methodology within GFEM partition of unity framework

A global-local (GL) method is a hybrid modeling or analysis technique, which consists of using some computational strategies to solve complex problems. Its application was driven by the demand of problems with physical and geometric nonlinearity (Noor, 1986).

The use of the global-local methodology with the GFEM consists of applying a zooming technique in which the solution of an isolated local problem is employed to numerically generate the enrichment of the global approximation space within the partition of unity framework; this association has been called Generalized Finite Element Method with Global-Local Enrichment (GFEM-GL). Unlike classical FEM applications, local-global interaction is possible when

GFEM is used; this gives us a good alternative to improve the global solution (Duarte and Kim, 2008).

The three fundamental steps in GFEM-GL are (figure 1):

1. Initially, a global problem is modeled with a coarse mesh.
2. Then, with the region of interest and the nodes to be enriched identified, one or more local problem(s) is (are) solved, using the solution of the first step as boundary conditions.
3. Finally, in the third step, we enrich the global problem, which could be processed again.

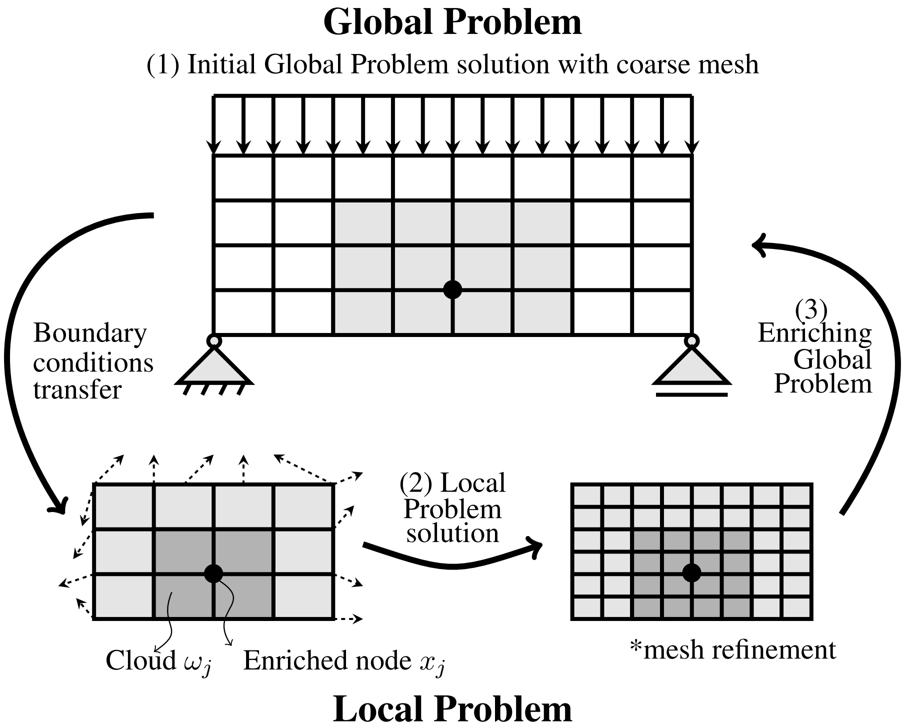

Figure 1: Global-Local steps. Adapted from Alves (2012).

3 FUNDAMENTALS OF THE PROPOSED MULTISCALE STRATEGY

In the present article, the association of the Global-Local methodology whith GFEM is proposed as a way of modeling problems in two levels, a coarse one (global) and a refined one (local). The introduction of the heterogeneity in the local level automatically characterizes the use of different scales of material observation, a macroscale (Global Problem) and a mesoscale (Local Problem) that transmits to the global domain its effects through the construction of the enrichment functions.

The proposed strategy could be classified, after de Borst et al. (2006), as follows: *Discretization methodology*: Coarse-to-refined; *Scales representation*: two scales (GFEM/GFEM or GFEM/ other method); *Continuity*: both scales are continuous; *Fine-scale boundary conditions*: Dirichlet/Neumman/Cauchy; *Interscale communication*: boundary conditions and enrichments (primarily).

3.1 Basic formulation

Boundary value problem to be modeled

Let $\Omega = \Omega_G \cap \Gamma_G$ be a domain in $\mathbb{R}^3$, whose boundary could be divided as $\Gamma_G = \Gamma_G^u \cup \Gamma_G^t$, with $\Gamma_G^u \cap \Gamma_G^t = \emptyset$. The following problem is introduced:

$$\nabla \cdot \boldsymbol{\sigma} = \mathbf{0}, \text{ in } \Omega_G \tag{6}$$
$$\mathbf{u} = \bar{\mathbf{u}}, \text{ on } \Gamma_G^u \tag{7}$$
$$\boldsymbol{\sigma} \cdot \mathbf{n} = \bar{\mathbf{t}}, \text{ on } \Gamma_G^t \tag{8}$$

in this way one could state:

Find $\mathbf{u}_G^k \in \mathbb{S}_G(\Omega_G) \subset H^1(\Omega_G) \mid \forall \ \delta\mathbf{u}_G^k \in \mathbb{S}_G(\Omega_G)$

$$\begin{aligned}\int_{\Omega_G} \nabla(\delta\mathbf{u}_G) : \boldsymbol{\sigma}(\mathbf{u}_G)\, dV + \eta \int_{\Gamma_G^u} \delta\mathbf{u}_G \cdot \mathbf{u}_G\, dS = \int_{\Omega_G} \delta\mathbf{u}_G \cdot \mathbf{b}\, dV + \int_{\Gamma_G^t} \delta\mathbf{u}_G \cdot \bar{\mathbf{t}}\, dS + \\ +\eta \int_{\Gamma_G^u} \delta\mathbf{u}_G \cdot \bar{\mathbf{u}}\, dS\end{aligned} \tag{9}$$

where η is a penalty parameter, $\bar{\mathbf{u}}$ and $\bar{\mathbf{t}}$ are prescribed displacements and tractions on the boundary, $\mathbf{n}$ is a vector normal to the surface Γ_G^t, $\mathbf{b}$ is the body forces vector and $\boldsymbol{\sigma} = \mathbf{D} : \boldsymbol{\epsilon}$, with $\mathbf{D}$ denoting a constitutive tensor, function of the strain field.

Local problem

Let $\mathbf{u}_G^k \in \mathbb{S}_G(\Omega_G)$ be a GFEM approximation for problem of equation 9 in the incremental step k. Prescribed boundary conditions $\bar{\mathbf{u}}^k$ and $\bar{\mathbf{t}}^k$ should be imposed in $(\Gamma_L \cap \Gamma_G^u)$ and $(\Gamma_L \cap \Gamma_G^t)$, respectively, using the boundary information. In $(\Gamma_L \backslash \Gamma_L \cap \Gamma_G)$, $\mathbf{u}_{G,0}$ is used as boundary conditions, where $\mathbf{u}_{G,0}^k := \mathbf{u}_{G,0}^k(\mathbf{u}_G^{k-1})$ is a function of the previous step solution. Therefore, the following problem can be addressed:

Find $\mathbf{u}_L^k \in \mathbb{S}_L(\Omega_L) \subset H^1(\Omega_L) \mid \forall \ \delta\mathbf{u}_L^k \in \mathbb{S}_L(\Omega_L)$

$$\begin{aligned}\int_{\Omega_L} \nabla\left(\delta\mathbf{u}_L^k\right) : \boldsymbol{\sigma}\left(\mathbf{u}_L^k\right) dV + \eta \int_{\Gamma_L \cap \Gamma_G^u} \delta\mathbf{u}_L^k \cdot \mathbf{u}_L^k dS + \kappa \int_{\Gamma_L \backslash (\Gamma_L \cap \Gamma_G)} \delta\mathbf{u}_L^k \cdot \mathbf{u}_L^k dS = \\ = \int_{\Omega_L} \delta\mathbf{u}_L^k \cdot \mathbf{b}^k dV + \int_{\Gamma_L \cap \Gamma_G^t} \delta\mathbf{u}_L^k \cdot \bar{\mathbf{t}}^k dS + \eta \int_{\Gamma_L \cap \Gamma_G^u} \delta\mathbf{u}_L^k \cdot \bar{\mathbf{u}}^k dS + \\ + \int_{\Gamma_L \backslash (\Gamma_L \cap \Gamma_G)} \delta\mathbf{u}_L^k \cdot \left[\mathbf{t}\left(\mathbf{u}_{G,0}^k\right) + \kappa\mathbf{u}_{G,0}^k\right] dS\end{aligned} \tag{10}$$

where $\boldsymbol{\sigma}$ is a nonlinear constitutive relation, $\left[\mathbf{t}\left(\mathbf{u}_{G,0}^k\right) + \kappa\mathbf{u}_{G,0}^k\right]$ represents stresses along the interface between local and global domains, which depends upon the initial global solution $(\mathbf{u}_{G,0}^k)$ and κ is a scalar chosen as to establish boundary conditions of Neumann ($\kappa = 0$), Dirichlet ($\kappa \cong \eta$) or Cauchy ($0 < \kappa < \eta$).

Global problem

The local solution $\mathbf{u}_L^k$ is used as a enrichment function numerically generated. Hence, the shape functions of GFEM are given as:

$$\phi_\alpha^k = N_\alpha \mathbf{u}_L^k \tag{11}$$

where the partition of unity is given by a relatively coarse FEM mesh in Ω_G. In that sense the following global problem is addressed:

Find $\mathbf{u}_G^k \in \mathbb{S}_G(\Omega_G) \subset H^1(\Omega_G) \ | \ \forall \ \delta\mathbf{u}_G^k \in \mathbb{S}_G(\Omega_G)$

$$\int_{\Omega_G} \nabla(\delta\mathbf{u}_G^k) : \hat{\boldsymbol{\sigma}}(\mathbf{u}_G^k)\, dV + \eta \int_{\Gamma_L \cap \Gamma_G^u} \delta\mathbf{u}_G^k \cdot \mathbf{u}_G^k\, dS = \int_{\Omega_G} \delta\mathbf{u}_G^k \cdot \mathbf{b}^k dV + \int_{\Gamma_L \cap \Gamma_G^t} \delta\mathbf{u}_G^k \cdot \bar{\mathbf{t}}^k dS + \\ + \eta \int_{\Gamma_L \cap \Gamma_G^u} \delta\mathbf{u}_G^k \cdot \bar{\mathbf{u}}^k dS \tag{12}$$

where $\hat{\boldsymbol{\sigma}}$ depends upon a constitutive tensor which is function of the local solution $\big(\mathbf{D} := \mathbf{D}(\mathbf{u}_L^k)\big)$ and is constant in the step k.

3.2 Description of the analysis procedures

Two scale nonlinear analysis

The goal is to divide the incremental-iterative analysis into two levels: the local one, in which the iterations of the nonlinear problem would be processed, and the global one in which incremental (load or displacement) steps would be performed. Thus, the local and refined instance is responsible for conducting the solution of the nonlinear spectrum of the analysis, while on the global scale, a linear (secant) problem is faced. The figure 2 illustrates the procedure. In this process, the boundary conditions of the local problems in a given step are obtained from the global solution of the previous step. Similar approach can be found in Kim and Duarte (2015), where it was used to tackle cohesive crack problems.

Multiscale strategy within GFEM framework

Next, the proposed analysis process is described, in accordance with the guidelines of the GFEM-GL and its nonlinear version. The figure 3 illustrates the multiscale strategy proposed in the paper.

Step 1 - Initial Global Problem: The macroscale domain is solved with the use of a coarse mesh. In this process, the global displacements are obtained to provide boundary conditions for the mesoscale. Other information such as damage evolution, stress, etc., may be necessary for the correct nonlinear analysis of the local problem(s). This procedure is called hereinafter downscaling (after Gitman et al. (2008)). In the context of GFEM-GL, this mechanism is based on a weak coupling between the global and local domains by means of the Penalty

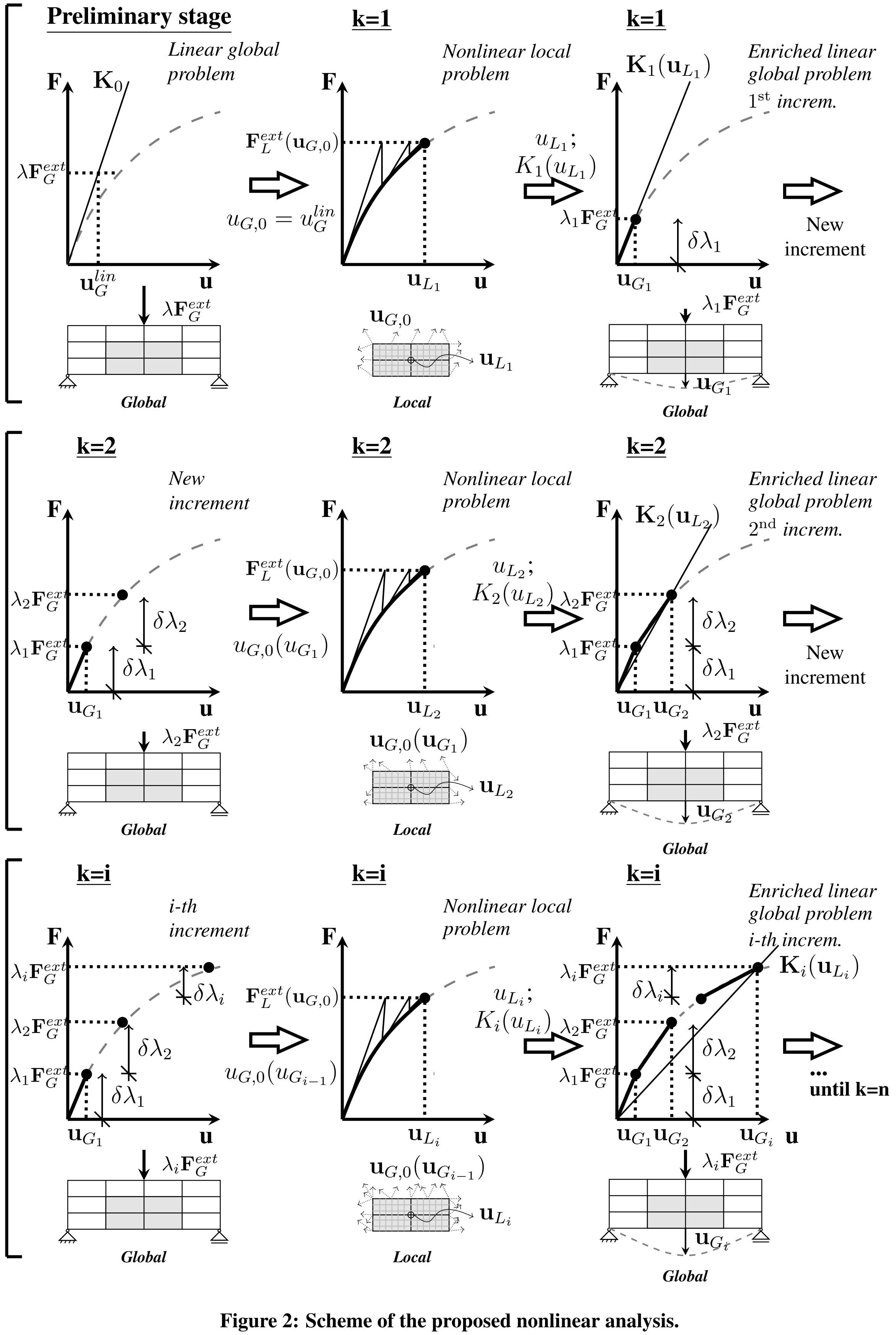

Figure 2: Scheme of the proposed nonlinear analysis.

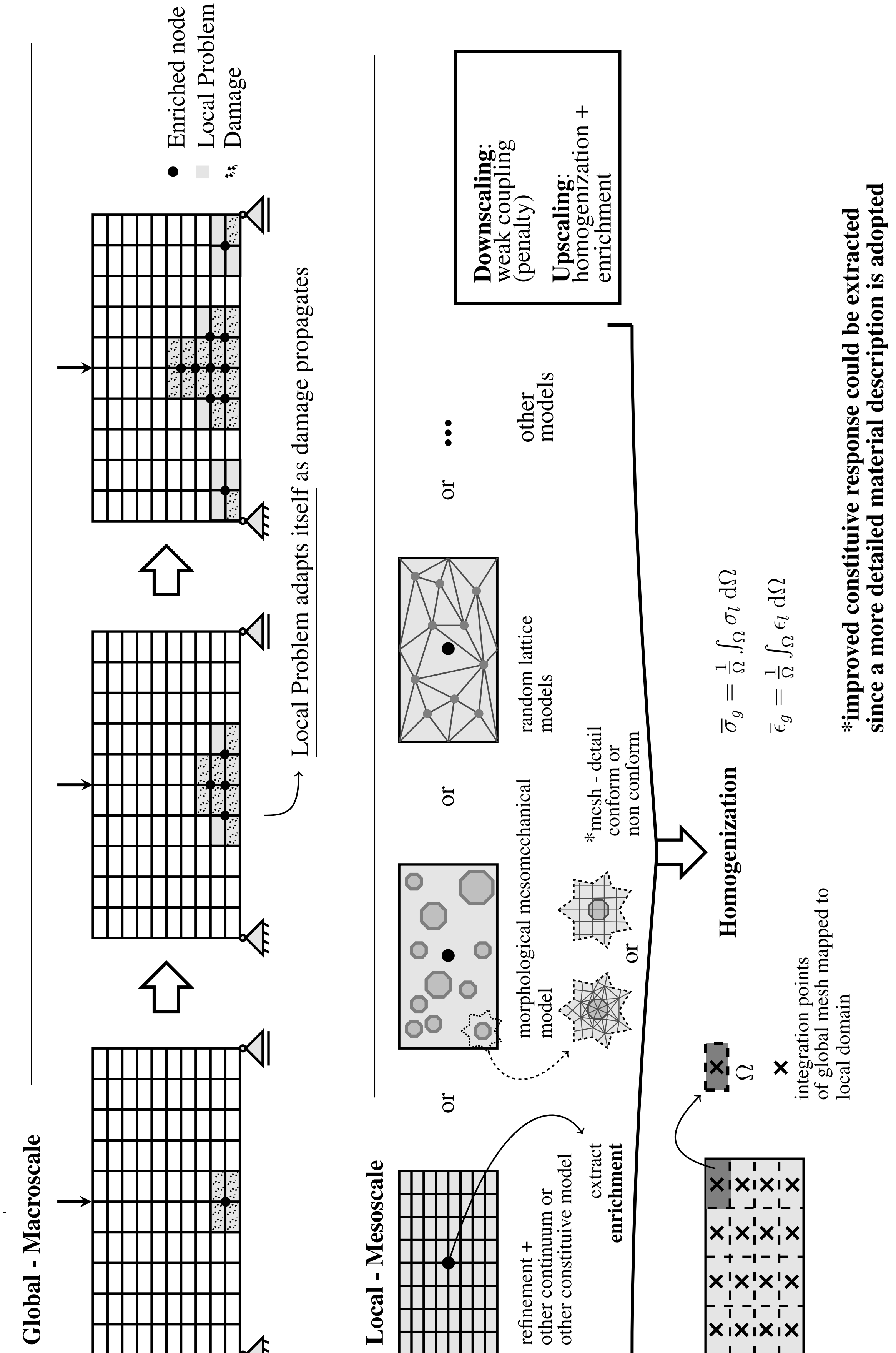

Figure 3: Scheme of the proposed multiscale strategy.

Method (Lagrange multipliers could also be used). This coupling, and the consequent passing of information, manifests itself in the transmission of boundary conditions from the Global Problem to the Local Problem, through the integration of state (and dual) variables along the interface between the domains.

Step 2 - Local problem(s): Once the solution of Step 1 is established, the solution of the local problems, which define the mesoscale, begins. In this step, nonlinear analysis are performed for each local problem, considering the heterogeneity of the medium and the consequent and intrinsic randomness of the properties in the domain. Once the solution of the first step is known, the local problem solution is independent, and thus, several local domains can be defined, respecting the prerogatives of the GFEM (the cloud of an enriched node must be inside the local domain). Thus, the parallelization of the solution process is one potential of GFEM-GL. We hope to develop an implementation that allows the maximum generalization of the local domain, that is, a code which enables the use of different (numerical) models for the Local Problem. Regarding the present work, we seek to represent the mesoscale using elastic degrading models in parallel with morphological mesomechanical models that describe the geometry of the internal configuration of the target material. In this step, the mechanism hereinafter called upscaling is defined (after Gitman et al. (2008)), in which two main procedures can be highlighted: homogenization and enrichment. A homogenization procedure ensures that the heterogeneous continuum, which describes the mesoscale, is translated into a homogeneous continuum, characteristic of the macroscopic scale (Gitman et al., 2008). This mechanism is used to obtain the global constitutive response of the material, in the regions in which the nonlinear mesoscopic analysis is activated. By mapping the global integration points of the macroscale mesh into the local domains, one could average the desired local variables (damage, stresses, strains etc.) in the volume around the point and integrate the global fixed mesh. On the other hand, the enrichment process is very straightforward, and consists of the extraction of displacements related to global enriched nodes to build GFEM shape functions as discussed previously.

Step 3 - Enriched Global Problem or Global-Local Problem: Reaching convergence at mesoscale, we proceed to Step 3. The current incremental step is over after the enrichment of the macroscale nodes with the solution of the local problem(s) and linear (secant) equilibrium of the Global Problem.

4 CURRENT STAGE OF THE RESEARCH

This work takes part in a much bigger project and the implementation of the above nonlinear algorithm and multiscale strategy within GFEM-GL is on its way now. The team architects the data structure to better fit the intended generalization and parallelization, and alternatives for the nonlinear global-local analysis are being tested. For now, the management of the morphological features of a particulate material have already been implemented and some examples are presented here. We emphasize the importance of this results, as they comprise a relevant part of the whole multiscale analysis proposed here. With a relatively good description of the internal morphology of the material, its possible to get an enhanced resolution of its behavior.

4.1 Mesostructure generator

The particles generator is based on – but not restricted to – Wriggers and Moftah (2006) and Wang et al. (1999). In this type of problem, a great effort is spent to deal with computational geometry aspects. To this matter, we sought not the perfect or most detailed way to describe the internal geometry, but a feasible approach capable to represent the material heterogeneity with less programming and computational exertion as possible. Besides that, in this type of algorithm the order of complexity increases fast as the problem is solved, i.e., as the number of particles grows, more tests need to be performed and more computational power is necessary.

The algorithm used (take-and-place algorithm) can be classified as a stochastic-heuristic process, that is, particles with random shapes (and/or sizes) and positions are placed one-by-one inside the analysis domain, and to each particle a number of checks is assigned in order to verify whether it can be placed or not; no overlapping is allowed, all created particles must be completely inside the domain and limiting distances ("particle-to-particle" and "particle-to-boundary") must be respected. These offsets are regulated by a distribution factor (DF) which enlarge the size of a particle before the execution of overlapping checkage.

Mesostructure plots

To illustrate the capacity of the matrix-heterogeneity mixture generator, it is presented different particle fraction (PF) distributions. The sizes of the particles are based on concrete aggregate specifications of ABNT NBR 7211 (2005) standard. Two types of particles were used, spherical and polygonal/irregular particles. For both genders, the particle characteristic dimension is taken as an average radius. So for the spherical ones the determination of a new particle is direct; as for the polygonal specimen, the creation of a particle is based on an average circumference circumscribed to a regular polygon (with PS sides) to which some angular and radial deviations are applied ($\Delta\alpha$ and ΔR). These variations represent how much a particle vertex deviates from one another and from the average radius, respectively, and were introduced to slightly roughen the particle.

The particles can be created using a continuous distribution or a specific grading curve obtained in laboratory. In the examples shown here, a Füller's curve was employed, for simplicity. This continuous function has the following form (Wriggers and Moftah, 2006):

$$P(d) = 100 \times \left(\frac{d}{d_{max}}\right)^n \tag{13}$$

where $P(d)$ is the percentage passing a sieve with size d; d_{max} is the maximum size of particles and n is a constant ($0.45 \leq n \leq 0.70$, according to Wriggers and Moftah (2006) and Wang et al. (1999)). The value of $n = 0.50$ was employed in this paper.

Next, we register some distribution examples inside a $10\,\mathrm{cm} \times 20\,\mathrm{cm}$ section. Typical particle fractions of concrete mixtures were selected – around 40% of coarse aggregates (Wang et al., 1999). In figure 4(a), 4(b) and 4(c), there are samples containing spherical particles and in figures 4(d), 4(e) and 4(f), polygonal inclusions are presented. All samples show a grading range typical of coarse aggregates – within the segment $25.0\,\mathrm{mm}$ to $4.75\,\mathrm{mm}$ (ABNT NBR 7211, 2005), except for figure 4(c) which presents particles all the way to fine sizes. The placement ratio (relation between the desired particle fraction and the actual fraction of placed particles) is around 99% in all examples.

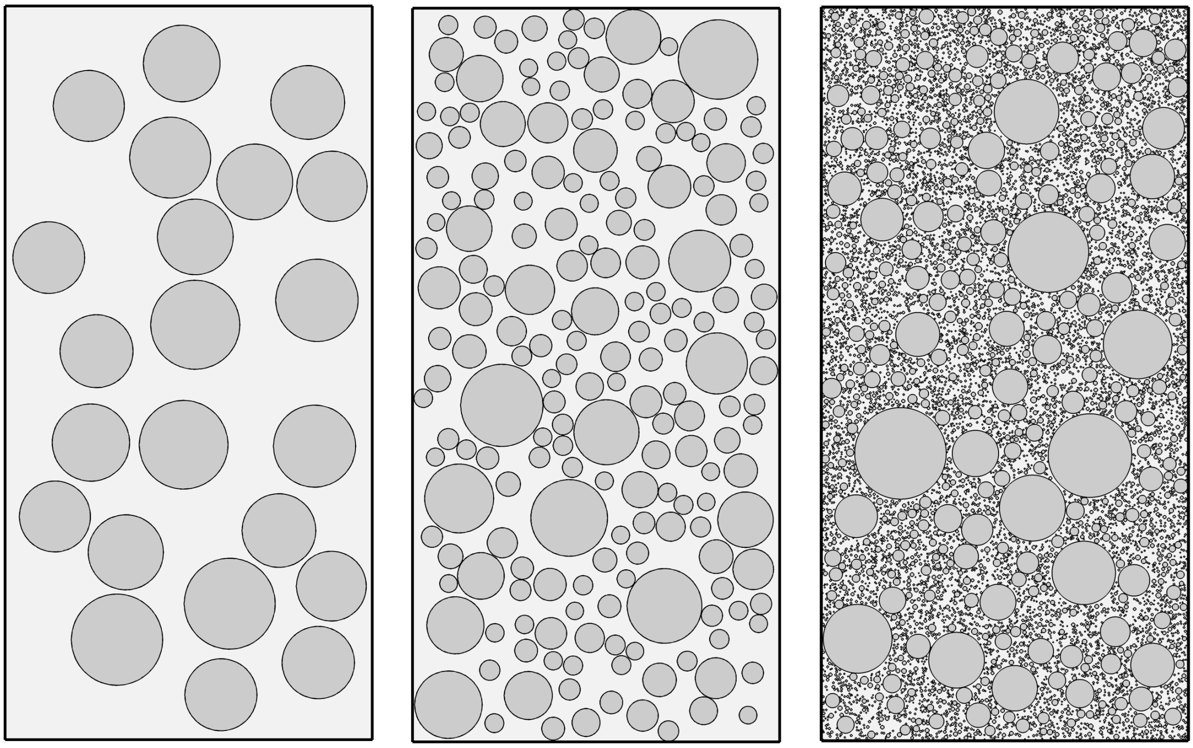

(a) $PF = 40\%; DF = 0.1; 25 - 19\,mm.$ (b) $PF = 50\%; DF = 0.02; 25 - 4.75\,mm.$ (c) $PF = 50\%; DF = 0.02; 25 - 0.030\,mm.$

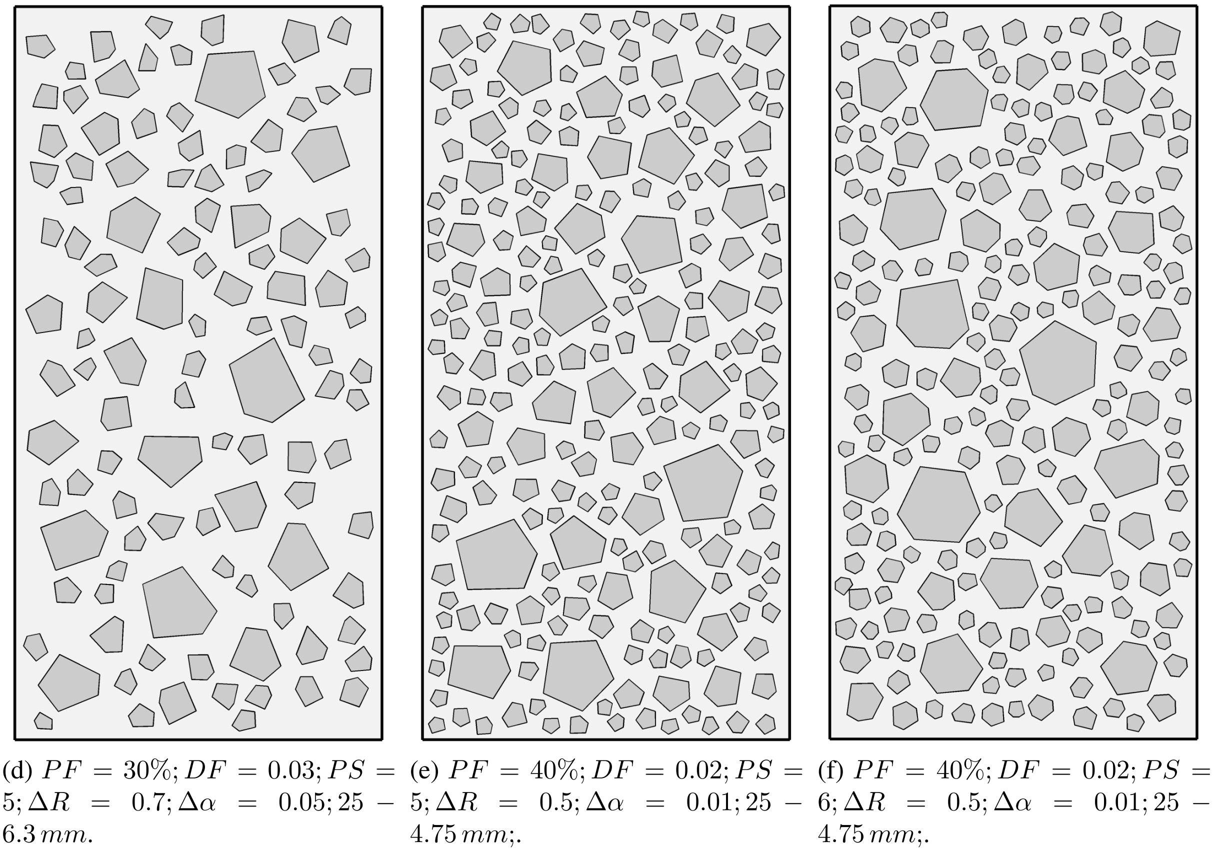

(d) $PF = 30\%; DF = 0.03; PS = 5; \Delta R = 0.7; \Delta\alpha = 0.05; 25 - 6.3\,mm.$ (e) $PF = 40\%; DF = 0.02; PS = 5; \Delta R = 0.5; \Delta\alpha = 0.01; 25 - 4.75\,mm;.$ (f) $PF = 40\%; DF = 0.02; PS = 6; \Delta R = 0.5; \Delta\alpha = 0.01; 25 - 4.75\,mm;.$

Figure 4: Morphology samples – spherical particles (4a), (4b) and (4c); polygonal particles (4d), (4e) and (4f).

4.2 Numerical example

For the numerical treatment of the geometric information from the particle distribution, we present here the so-called FEM pixel approach (Bohm, 2016). In this strategy, it is used a non-conform mesh (not aligned to the geometry) and the material information of a entire finite element is chosen based on whether the element barycenter lies inside a particle or not (assignment of particle/aggregate properties or matrix properties). The mesh should be fine enough to capture the geometry variation of the particles.

Mesostructure numerical treatment

We propose here a simple linear problem, in plane stress, in which there are rigid inclusions embedded in a elastic matrix ($E_{particle} \gg E_{matrix}$). This choice of material properties was made in order to increase the heterogeneity effects on the problem. Thereby, a direct mesostructural simulation was carried out using the previous mentioned numerical model. Spherical particles and a fixed grading segment were employed. Three different simulations of the heterogeneous problem were performed (figures 7, 8 and 9), as well as the processing of a homogeneous reference case (figure 6). In that sense, the following problem is presented (figure 5):

Material ($E_{particle} \gg E_{matrix}$)
$E_{matrix} = 30\,\mathrm{GPa}$, $\nu_{matrix} = 0.2$
$E_{particle} = 10 \times E_{matrix}$, $\nu_{particle} = 0.2$
Geometry (cm) and Boundary Conditions
$h = 10.0, w = 20.0, t = 1.0$
$p = 1.0kN/cm^2$; left/bottom sides fixed
Particle distribution
$PF = 20\%; DF = 0.3; 19.0 - 12.5\,mm$

(a) Input parameters.

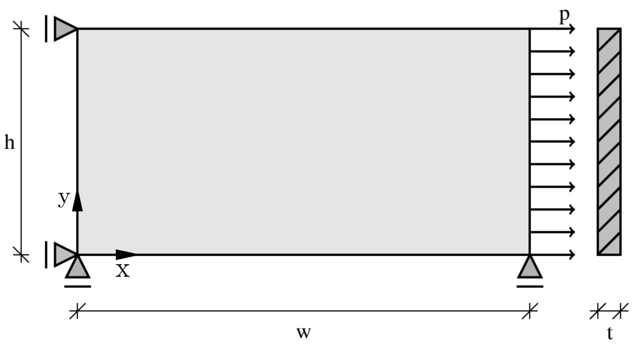

(b) Model.

Figure 5: Numerical example.

Results from three different mesostructural simulations are shown next. Even though the problem is kept the same, the stochasticity of the material heterogeneity manifests itself and pervades the model behavior. Figure 6 presents the FEM mesh used in the examples and the results of a homogeneous problem. Figures 7, 8 and 9 show three simulations and the respective responses of each one. Since in the proposed test the predominant fields are in the x–direction we chose to register the contour of these variables – images (b), (c) and (d) of each figure. The maximum and minimal values of each field are highlighted in the picture caption ($d_x^{max}, \epsilon_{xx}^{max}, \epsilon_{xx}^{min}, \sigma_{xx}^{max}, \sigma_{xx}^{min}$). As it can be seen, the consideration of a heterogeneous continuum to model the problem, highly affects the results. The expected homogeneous fields of a pure traction test are not observed when a matrix-particle dispersion is considered. In figures 7, 8 and 9, images (c) and (d), patterns of potential failure regions, which could govern the material behavior – especially localizing continua (when considered), can be identified. In general, strain and stress tend to concentrate in the inclusion boundary and in between particles.

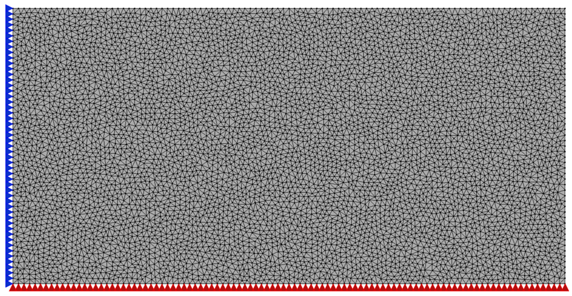

(a) Mesh used in all simulations (average size = 0.2 cm). 3-noded triangular element.

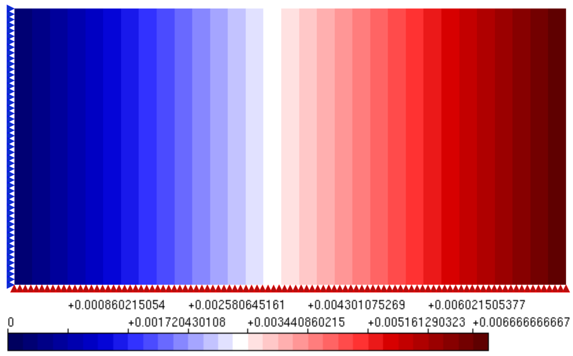

(b) Displacement d_x (cm). $d_x^{max} = 6.66 \times 10^{-3}$.

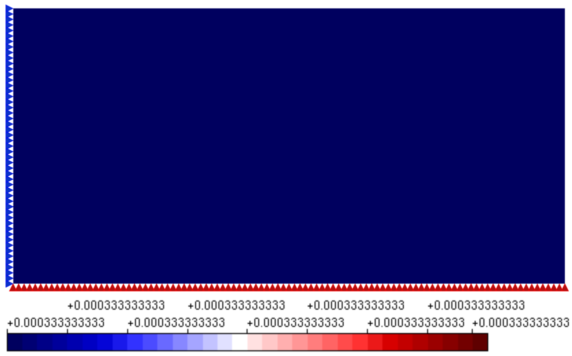

(c) Strain ϵ_{xx} (cm/cm). $\epsilon_{xx}^{max} = 3.33 \times 10^{-4}$ (constant).

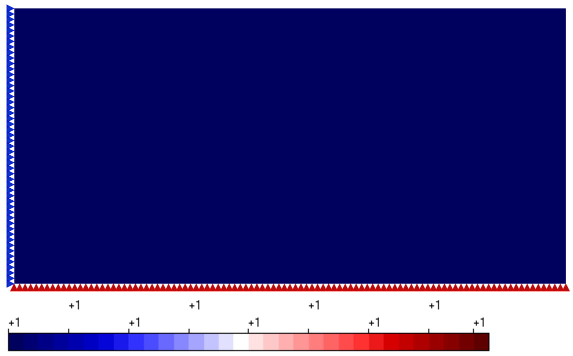

(d) Stress σ_{xx} (kN/cm^2). $\sigma_{xx}^{max} = 1.00$ (constant).

Figure 6: Finite element mesh and reference problem (homogeneous case).

5 FINAL REMARKS

The theoretical basis of a different multiscale approach was presented. In this strategy, one relies on the partition of unity framework within the GFEM and uses a specific type of enrichment procedure (global-local enrichment) in order to capture localized features and behaviors inside the analysis domain. Here, we have proposed the generalization of the GFEM-GL local problem and the introduction of material morphological information within the mesolevel. With that, we seek to enhance the material description and to improve the overall structural response. Some results of the current stage were also shown. The mesostructure generator can deal with different particle fractions and geometries and embodies the influence of heterogeneity randomness in the global response. Since every new simulation is a completely new problem, even if the input parameters are the same, the computational model tends to emulate better the expected behavior obtained in real experiments. The next stage of this research will deal with the implementation of other numerical treatments to solve the mesoscale (e.g., usage of conform meshes, multiphase elements, among others) and the introduction of these processes in the proposed nonlinear analysis.

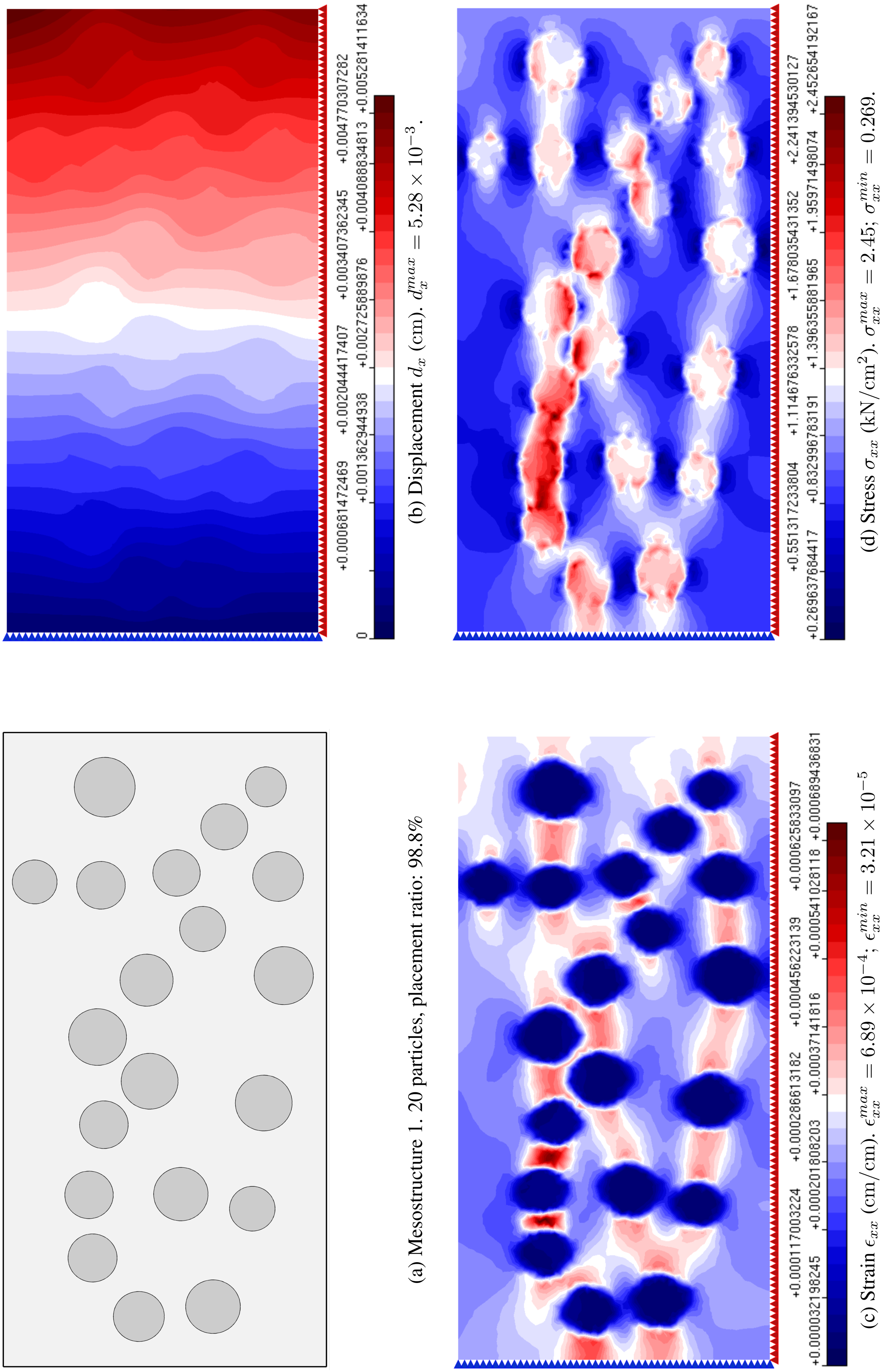

(a) Mesostructure 1. 20 particles, placement ratio: 98.8%

(b) Displacement d_x (cm). $d_x^{max} = 5.28 \times 10^{-3}$.

(c) Strain ϵ_{xx} (cm/cm). $\epsilon_{xx}^{max} = 6.89 \times 10^{-4}$; $\epsilon_{xx}^{min} = 3.21 \times 10^{-5}$

(d) Stress σ_{xx} (kN/cm^2). $\sigma_{xx}^{max} = 2.45$; $\sigma_{xx}^{min} = 0.269$.

Figure 7: Example 1: morphology (7a), displacement in x–direction (7b), strain in x–direction (7c) and stress in x–direction (7d).

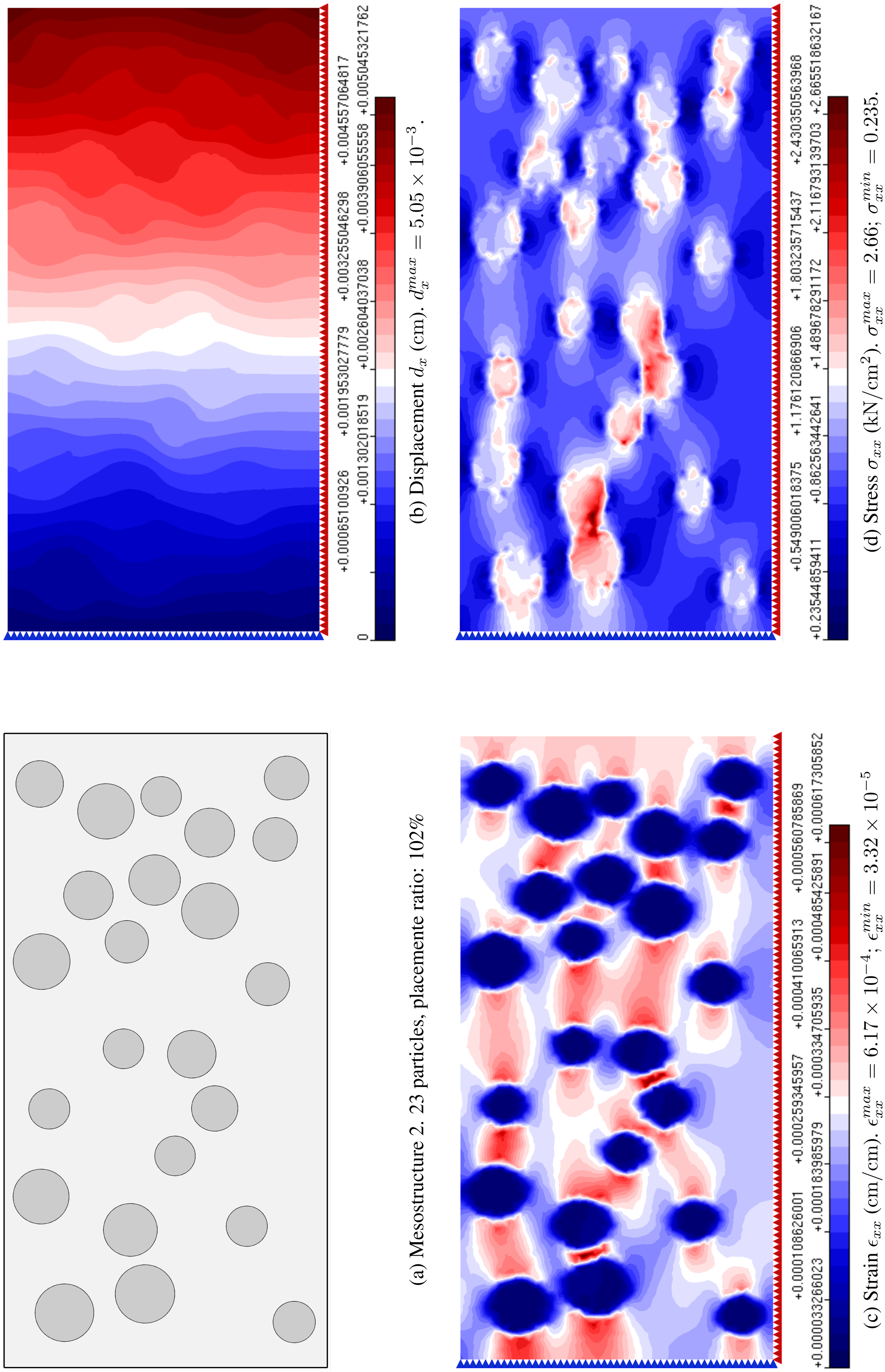

(a) Mesostructure 2. 23 particles, placemente ratio: 102%

(b) Displacement d_x (cm). $d_x^{max} = 5.05 \times 10^{-3}$.

(c) Strain ϵ_{xx} (cm/cm). $\epsilon_{xx}^{max} = 6.17 \times 10^{-4}$; $\epsilon_{xx}^{min} = 3.32 \times 10^{-5}$

(d) Stress σ_{xx} (kN/cm^2). $\sigma_{xx}^{max} = 2.66$; $\sigma_{xx}^{min} = 0.235$.

Figure 8: Example 2: morphology (8a), displacement in x–direction (8b), strain in x–direction (8c) and stress in x–direction (8d).

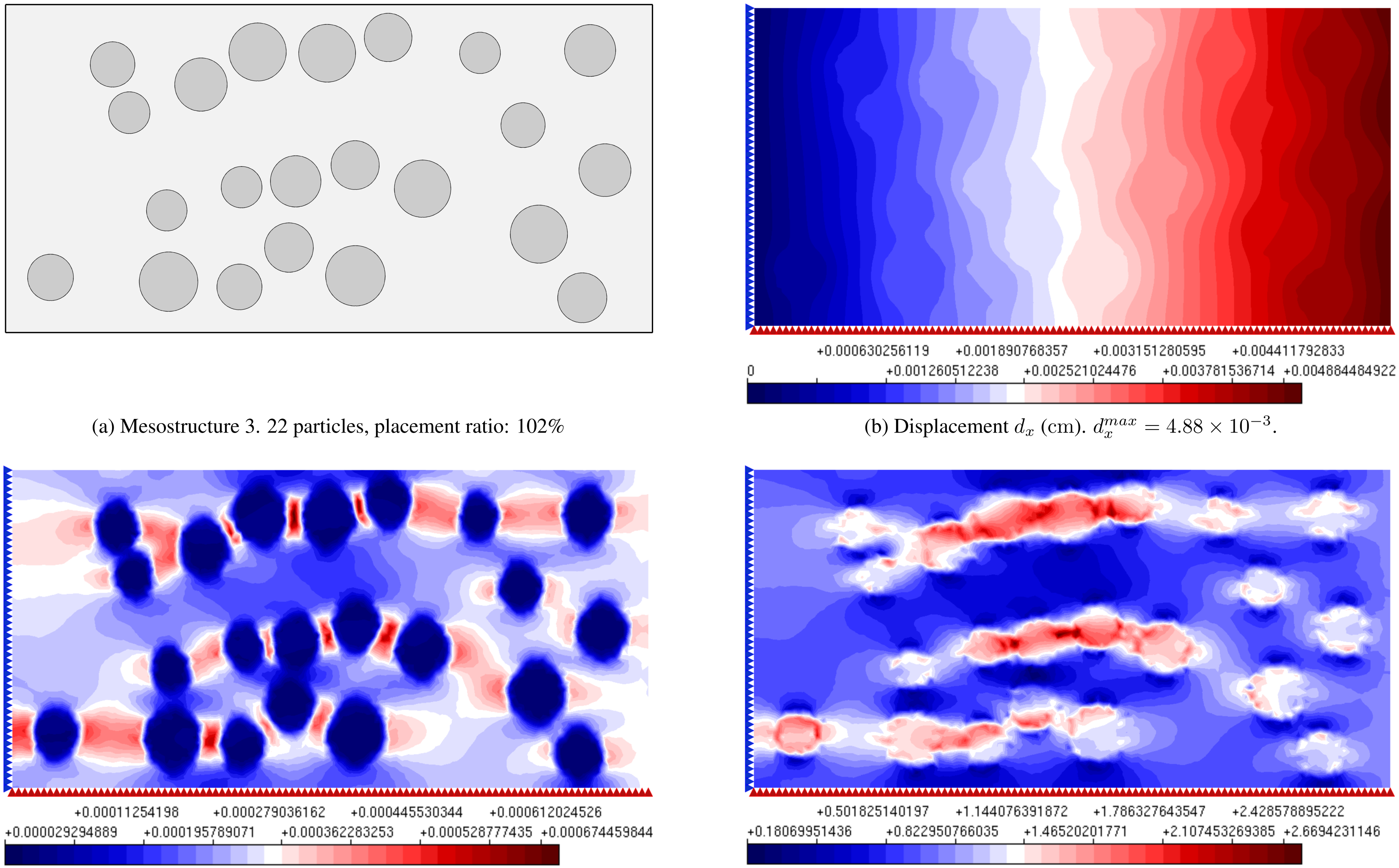

(a) Mesostructure 3. 22 particles, placement ratio: 102%

(b) Displacement d_x (cm). $d_x^{max} = 4.88 \times 10^{-3}$.

(c) Strain ϵ_{xx} (cm/cm). $\epsilon_{xx}^{max} = 6.74 \times 10^{-4}$; $\epsilon_{xx}^{min} = 2.92 \times 10^{-5}$

(d) Stress σ_{xx} (kN/cm^2). $\sigma_{xx}^{max} = 2.67$; $\sigma_{xx}^{min} = 0.181$.

Figure 9: Example 3: morphology (9a), displacement in x–direction (9b), strain in x–direction (9c) and stress in x–direction (9d).

Acknowledgments

The authors are grateful for the financial support granted by the National Council for Scientific and Technological Development (in Portuguese, Conselho Nacional de Desenvolvimento Científico e Tecnológico – CNPq), by the Coordinating Body of Graduate Personnel Development (in portuguese, Coordenação de Aperfeiçoamento de Pessoal de Nível Superior – CAPES) and by the Research Support Foundation of Minas Gerais (in Portuguese, Fundação de Amparo à Pesquisa do Estado de Minas Gerais – FAPEMIG). Furthermore, we would like to thank Professor Samuel Silva Penna (Department of Structural Engineering, Federal University of Minas Gerais) for the discussions and contributions to the implementation of the material morphology generator.

REFERENCES

ABNT NBR 7211, 2005. ‘Agregados para concreto – especificação’. *Associação Brasileira de Normas Técnicas*, p. 11.

Alves, P. D., 2012. Estratégia global-local aplicada ao método dos elementos finitos generalizados. Master Thesis, Universidade Federal de Minas Gerais, Belo Horizonte, MG, Brasil.

Babuška, I., Caloz, G. and Osborn, J. E., 1994. ‘Special finite element methods for a class of second order elliptic problems with rough coefficients’. *SIAM Journal on Numerical Analysis*, vol. 31(4), pp. 945–981.

Barros, F. B., 2002. Métodos Sem Malha e Método dos Elementos Finitos Generalizados em Análise Não Linear de Estruturas. phdthesis, Universidade de São Paulo.

Bohm, H. J., (2016), A short introduction to basic aspects of continuum micromechanics, techreport ILSB Report 206, ILSB-Vienna University of Technology. year 1998. updated january 25, 2016.

de Borst, R., Hulshoff, S. J., Lenz, S., Munts, E. A., van Brummelen, H. and Wall, W. A., (2006), Multiscale methods in computational fluid and solid mechanics, *in* E. O. P. Wesseling and J. Périaux, eds, ‘European Conference on Computational Fluid Dynamics - ECCOMAS CFD’, p. 18.

Duarte, C., 2001. ‘A generalized finite element method for the simulation of three-dimensional dynamic crack propagation’. *Computer Methods in Applied Mechanics and Engineering*, vol. 190(15-17), pp. 2227–2262.

Duarte, C. A., (1995), A review of some meshless methods to solve partial differential equations, techreport, TICAM - Texas Institute for Computational and Applied Mathematics, The University of Texas at Austin. Taylor Hall 2.400. Austin, Texas, 78712, U.S.A.

Duarte, C. A. and Babuška, I. M., (2005), A global-local approach for the construction of enrichment functions for the generalized fem and its application to propagating three-dimensional cracks, *in* ‘ECCOMAS Thematic Conference on Meshless Methods’.

Duarte, C. A. and Oden, J. T., 1996*a*. ‘H-p clouds–an h-p meshless method’. *Numerical Methods for Partial Differential Equations*, vol. 12(6), pp. 673–705.

Duarte, C., Babuška, I. and Oden, J., 2000. 'Generalized finite element methods for three-dimensional structural mechanics problems'. *Computers & Structures*, vol. 77(2), pp. 215–232.

Duarte, C. and Kim, D.-J., 2008. 'Analysis and applications of the generalized finete element method with global-local enrichment functions'. *Computer Methods in Applied Mechanics and Engineering*, vol. 197(6-8), pp. 487–504.

Duarte, C. and Oden, J., 1996*b*. 'An h-p adaptive method using clouds'. *Computer Methods in Applied Mechanics and Engineering*, vol. 139(1-4), pp. 237–262.

Fries, T.-P. and Belytschko, T., 2010. 'The extended/generalized finite element method: An overview of the method and its applications'. *International Journal for Numerical Methods in Engineering*, .

Fuina, J., da Silva Pitanqueira, R. L. and Penna, S. S., 2010. 'Contínuos generalizados: de voigt à modelagem de materiais parcialmente frágeis'. *Semina: Ciências Exatas e Tecnológicas*, vol. 31(2), pp. 119–130.

Gitman, I., Askes, H. and Sluys, L., 2008. 'Coupled-volume multi-scale modelling of quasi-brittle material'. *European Journal of Mechanics - A/Solids*, vol. 27(3), pp. 302–327.

Gori, L., Penna, S. S. and Pitangueira, R. L. S., 2017. 'A computational framework for constitutive modelling'. *Computers and Structures*, vol. 187, pp. 1–23.

Gupta, V., Duarte, C., Babuška, I. and Banerjee, U., 2015. 'Stable GFEM (SGFEM): Improved conditioning and accuracy of GFEM/XFEM for three-dimensional fracture mechanics'. *Computer Methods in Applied Mechanics and Engineering*, vol. 289, pp. 355–386.

Karihaloo, B., 2010. 'What is quasi-brittle fracture and how to model its fracture behaviour'. *The FESI Bulletin: International Magazine on Engineering Structural Integrity*, vol. 4(4).

Kim, D.-J. and Duarte, C., (2009), Generalized finite element method with global-local enrichments for nonlinear fracture analysis, *in* H. da Costa Mattos and M. Alves, eds, 'Mechanics of Solids in Brazil', Brazilian Society of Mechanical Sciences and Engineering, pp. 319–330.

Kim, D.-J., Duarte, C. A. and Proenca, S. P., 2012. 'A generalized finite element method with global-local enrichment functions for confined plasticity problems'. *Computational Mechanics*, vol. 50(5), pp. 563–578.

Kim, D.-J., Duarte, C. A. and Sobh, N. A., 2010. 'Parallel simulations of three-dimensional cracks using the generalized finite element method'. *Computational Mechanics*, vol. 47(3), pp. 265–282.

Kim, D.-J., Pereira, J. P. and Duarte, C. A., 2009. 'Analysis of three-dimensional fracture mechanics problems: A two-scale approach using coarse-generalized FEM meshes'. *International Journal for Numerical Methods in Engineering*, vol. 81, pp. 335–365.

Kim, J. and Duarte, C. A., 2015. 'A new generalized finite element method for two-scale simulations of propagating cohesive fractures in 3-D'. *International Journal for Numerical Methods in Engineering*, vol. 104(13), pp. 1139–1172.

Melenk, J. and Babuška, I., 1996. 'The partition of unity finite element method: Basic theory and applications'. *Computer Methods in Applied Mechanics and Engineering*, vol. 139(1-4), pp. 289–314.

Melenk, J. M., 1995. On Generalized Finite Element Methods. Phd Thesis, University of Maryland.

Noor, A. K., 1986. 'Global-local methodologies and their application to nonlinear analysis'. *Finite Elements in Analysis and Design*, pp. 333–346.

Plews, J. A. and Duarte, C. A., 2016. 'A two-scale generalized finite element approach for modeling localized thermoplasticity'. *Int. J. Numer. Meth. Engng*, .

Plews, J. and Duarte, C., 2014. 'Bridging multiple structural scales with a generalized finite element method'. *International Journal for Numerical Methods in Engineering*, vol. 102(3-4), pp. 180–201.

Ransom, J. B. and N. F. Knight, J., (1989), Global/local stress analysis of composite panels, techreport NASA-TM-101622, NASA, Langley Research Center. Hampton, Virginia.

Wang, Z., Kwan, A. and Chan, H., 1999. 'Mesoscopic study of concrete i: generation of random aggregate structure and finite element mesh'. *Computers & Structures*, vol. 70(5), pp. 533–544.

Wriggers, P. and Moftah, S., 2006. 'Mesoscale models for concrete: Homogenisation and damage behaviour'. *Finite Elements in Analysis and Design*, vol. 42(7), pp. 623–636.

Zienkiewicz, O. C., Taylor, R. L. and Zhu, J. Z., 2006, *The Finite Element Method*, 6 edn, Elsevier, chapter 18 - Multiscale modeling, pp. 547–589.